Experiments in Fluids 13, 26–32 (1992)

Experiments in Fluids

Computer-based areal surface temperature and local heat transfer measurements with thermochromic liquid crystals (TLC)

K.-H. Platzer, C. Hirsch, D. E. Metzger* and S. Wittig

Lehrstuhl u. Institut für Thermische Strömungsmaschinen, Universität Karlsruhe (T.H.) D-7500 Karlsruhe, FRG

Abstract. The experimental technique presented is designed to obtain detailed local heat transfer data on both stationary as well as rotating disc-cavity surfaces applicable to gas turbines. The method employed utilizes thin coatings of thermochromic liquid crystals (TLC) as surface temperature indicators under aerodynamically steady but thermally transient experimental conditions. The color display of the liquid crystals is monitored by a video camera. The video signals are captured in real time by a computer-based color recognition system to extract areal temperature and heat transfer information. Some typical results are presented and compared with literature data to illustrate the potential of the system.

List of symbols

Symbols	Unit	Physical property
a	m^2/s	thermal diffusivity
B	–	blue color signal
G	–	green color signal
G	–	rotor/stator spacing ratio z/r_0
Nu_{r0}	–	Nusselt number $\alpha r_0/\lambda$
r	m	radial location
r_0	m	disc radius
R	–	red color signal
Re_m	–	mass flow Reynolds number $\dot{V}/2\pi z \nu$
Re_{r0}	–	rotational Reynolds number $\omega r_0^2/\nu$
t	s	time
T_0	K	initial temperature
T_{ref}	K	convecting fluid temperature
T_s	K	disc surface temperature
U	–	color difference signal
V	–	color difference signal
Y	–	luminance signal
z	m	rotor/stator spacing
α	–	spectral weight factor
α	W/m^2K	local heat transfer coefficient
β	1/K	volumetric expansion coefficient
β	–	spectral weight factor
δ	–	scaling factor
δ_{ij}	–	Kronecker-Delta
ε	–	scaling factor
γ	–	spectral weight factor
λ	W/mK	thermal conductivity
ν	m^2/s	fluid kinematic viscosity
ϱ	kg/m^3	fluid density

* Present address: Arizona State University, Tempe, AZ, USA

1 Introduction

The optimization of heavily loaded gas turbine components is a central topic in the research activities at the Institute for Thermal Turbomachinery (ITS), University of Karlsruhe. Particularly for jet engine applications, the thermal stress of the components is of special importance. Therefore, numerous techniques for heat transfer measurement have been developed or adapted to the specific measurement task. Besides the combustion chamber and blades, the turbine rotor discs have also to be considered as components under high thermal and mechanical stress. The lateral surfaces of the rotor discs represent a special problem with respect to heat transfer measurement because of the difficult accessibility.

Thermochromic Liquid Crystals (TLC) offer several advantages as local surface temperature indicators in such applications:

- The experimental setup is less complex compared to techniques previously used (Dibelius et al. 1984; Owen 1984).
- Because of its principle, this technique yields areal information. Therefore, not only integral but also local heat transfer coefficients can be determined and thermal stress information can be made available for every point of the component's surface.

If non-steady measurement techniques are employed, the time requirements can be significantly reduced, especially for parameter variations. In this context, after a sudden change in free stream temperature, it is necessary to determine the precise times when the individual points of the monitored surface reach a certain temperature. This temperature is indicated by a specific hue of the TLC coating.

The selectivity of the detection system with respect to this colour hue can be achieved by optical methods (monochrome system), but it is also possible to capture the full colour information and to perform the colour comparison by computer-based image processing techniques. In this case, even several temperatures can be monitored simultaneously, providing the opportunity to reduce uncertainties and to increase reproducibility.

In the research program presented in this paper, a rotor/stator system has been selected as a test case for the TLC method because of its importance for gas turbine design. The measurement technique implemented at the ITS using real time true color detection will now be described in detail.

2 Thermochromic liquid crystals

Materials that show a so-called mesophase during the transition from solid state to the isotropic liquid state are commonly named liquid crystals (LC). In this mesopahse state, liquid crystals exhibit a macroscopically liquid behavior, but they still possess distinct solid characteristics, for example double refraction (Oseen 1933).

Thermochromic liquid crystals (TLC) selectively reflect incident light depending on their temperature. Because of this property, a reversible color change occurs that is highly reproducible.

2.1 Optical and thermal properties

This effect is caused by double refraction: the incident light is split into two linearly polarized waves in orthogonal planes that propagate with different velocities along the optical axis. When they leave the crystal, the two waves superpose, leading to a rotation of the polarization plane (Vries 1951).

When the crystals are heated, the molecular geometry of the helical structure shown in Fig. 1 changes: the pitch P of the helix is increased, leading to longer reflected wavelengths. At the same time, however, the displacement angle Θ grows, resulting in a reduction of the wavelength. In most TLC materials, this second effect dominates so that the reflected light spectrum is shifted from long to short wavelengths with increasing temperature.

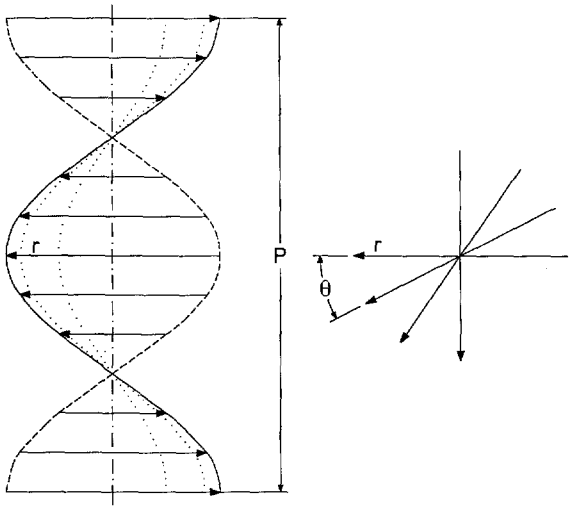

Fig. 1. Structure of the TLC-crystals

2.2 Local resolution and response time

Pure TLC materials show a temperature step response time of the order of 0.1 s. Their local resolution limit in a temperature field is approximately 10 μm.

These values of response time and spatial resolution are affected by the thermal properties of the substrate where the TLC coating is applied, particularly if the thermal conductivity of TLC-film and substrate are significantly different. If the TLC material is micro-encapsulated, as is commonly the case, the heat capacity of the capsule material also lengthens the response time and reduces the local resolution. Finally, the thickness of the TLC coating and its contact with the substrate can also affect the accuracy of temperature measurement.

Because of the TLC coating's layered structure, the selective reflection is superposed onto refraction effects, causing the reflected wavelength λ to be dependent on both the incidence angle Θ_I of the illumination and the observation angle Θ_S. This relationship can be described by the formula

$$\lambda = \lambda_n \cos \frac{1}{2}\left[\sin^{-1} \frac{\sin \Theta_I}{n} + \sin^{-1} \frac{\sin \Theta_S}{n} \right] \quad (1)$$

where n is the average index of refraction of the liquid crystal and λ_n is the peak wavelength obtained from light travelling along the helical axis (Elser and Ennulat 1976). Therefore, shorter wavelengths (i.e., colours shifted to blue) are observed for increasing angles. However, disturbing effects due to direct reflection of light at the surface also have to be taken into account (Böttcher 1972).

During our experiments, we were able to observe optimum results with encapsulated TLC coatings of approx. 20 μm thickness, when the illumination angle Θ_I was about 30° to the surface normal and the camera was positioned normally to the test surface ($\Theta_S = 0°$).

2.3 Handling of TLC coatings

Micro-encapsulated TLC offer significant advantages in handling compared with pure TLC (Hirsch 1987b). By enclosing TLC droplets within a thin polymer cover, tiny spheres with diameters in the range o 10 to 50 μm are created that are commercially available in a suspension.

The TLC material we used for our experiments (Merck/BDH) can be applied both by using a brush and spraying. In both cases, the quality of the coating is best if the crystals are heated above the detection temperature range before applying them to the substrate, because of the better viscous properties at higher temperature. When a plexiglass substrate is used, we found it advantageous to roughen the surface by sandblasting to ensure that the active surface for wetting is sufficiently large to achieve good adhesion.

The best colour contrasts can be achieved using a black, absorbing substrate. However, in spite of encapsulation, the

TLC seem to react with the components of some paints, making it impossible to apply TLC coatings directly to certain painted surfaces. Aluminium components can be treated by the eloxal process; for transparent plexiglass parts it is often sufficient to blacken the reverse side that is not in contact with the TCL material.

3 Data acquisition and analysis

A computer-based color detection and image processing system has been developed to perform the quantitative interpretation of the TLC color display. A major requirement for the system was the capability for real time acquisition and processing of the video information: the system's resolution in time had to be fast enough to minimize uncertainties in the determination of the heat transfer coefficients when investigating step responses in non-steady experiments.

3.1 Principle of color recognition

3.1.1 RGB system

Because the TLC surface is scanned by a video camera during digital image processing, the way the color signal is transferred in color TV seems to be a natural choice for the design of a color recognition system.

In a TV receiver, a color picture is generated by additive superposition of three primary colors: red, green and blue (RGB system). Each pixel is characterized by a triplet of RGB intensities, the color vector $\vec{c}$. The length of this vector indicates the brightness and its orientation in the three-dimensional cartesian RGB system indicates the color. A specific color hue corresponds to a fixed relation of these vector components (Seidel and Burlisch 1986).

During the interpretation of TLC data, only this color hue and not the intensity is of interest. Therefore the color recognition can be restricted to testing the collinearity of the measured color vector $\vec{c}$ with a reference vector $\vec{c}_0$. Using this approach, informations on three colors have to be simultaneously digitized to perform a unique color detection. This results in very demanding hardware requirements.

3.1.2 YUV system

However, both the complexity of the color recognition system and its cost may be significantly reduced if a different reference coordinate system for the color vectors is employed. Again, there is an analogy to the current transmission process for color TV signals: to maintain compatibility with *b/w* TV receivers, color-independent information, the so-called luminance Y (brightness) is generated by a transformation defined by:

$$Y \equiv \alpha R + \beta G + \gamma B$$

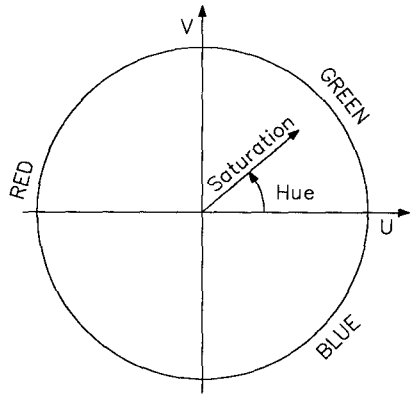

Fig. 2. Color circle in the UV system

with

$$\alpha + \beta + \gamma = 1$$

Here, α, β and γ are weighting factors that are derived from the spectral sensitivity of the human eye for the primary colors. Using this luminance, two color-difference signals U and V can be created:

$$U = \delta(R - Y)$$
$$V = \varepsilon(B - Y)$$

with $\delta, \varepsilon > 0$

As mentioned, Y is color-independent and contains only monochrome (brightness) information, with all color information contained in U and V. These two color differences can be interpreted as the components of a color vector $\vec{r}(U, V)$ in a two-dimensional cartesian coordinate system, where the direction of the vectors stands for the color hue and its length for the color saturation. Colors of the same saturation are located at circles around the origin (Fig. 2). In the center of this color circle, the color is unsaturated; this corresponds to black, grey or white depending on the luminance. As a whole, the cylindrical coordinate system for hue, saturation and intensity (HSI system) can be used to replace the cartesian RGB system with only two color-dependent parameters.

3.2 Computer-based image processing

The digital data acquisition and image processing system is shown in Fig. 3. A commercial CCD video camcorder is used. In its so-called FBAS output signal, brightness and color information is encoded similar to the YUV system described above. In a color monitor, this multiplexed FBAS signal is decoded, yielding luminance and color information once more. The color difference signals U, V and a synchronization pulse are connected to a PC/AT computer system equipped with two real time image processing interfaces (frame grabbers). Because these frame grabber interfaces are

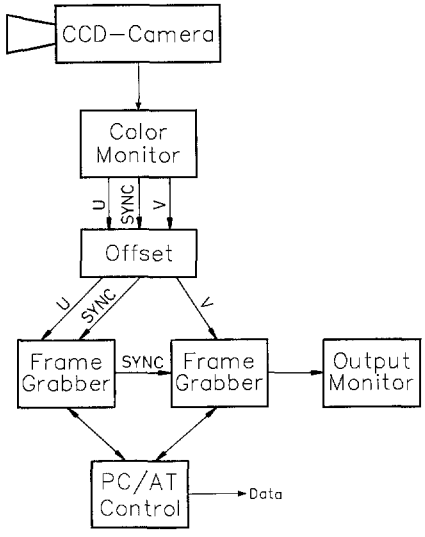

Fig. 3. Digital image-processing system

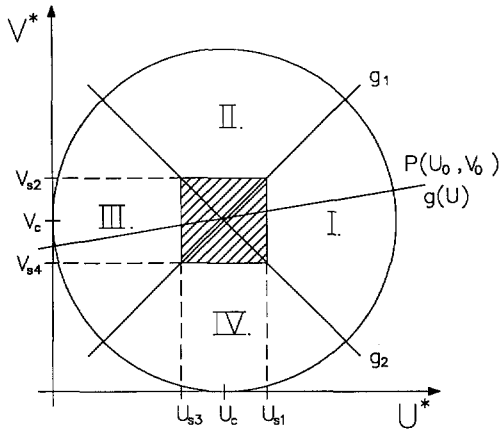

Fig. 4. Color detection, sector method

designed to capture unipolar CCIR-standard video signals, an interface circuit is used to add an offset voltage to the bipolar U, V difference signals to avoid negative signal voltages. In this circuit, a reference voltage present in ordinary CCIR signals, the so-called black shoulder, is also blended into the U, V signals.

The digitized color difference signals are stored in the frame grabbers' local memories of $512 \times 512 \times 8$ bits each that are mapped into the PC's address space and, therefore, can be accessed by the color detection software. Due to performance considerations, only 25% of the video picture (256×256 pixels) is used for color detection. An averaging is performed over an area of 4×4 pixels, finally leading to an array of 64×64 points which are continuously checked for the pre-defined color hue in every cycle of the color detection program.

3.3 Color-detection algorithm

Based on the YUV color representation, algorithms for efficient colour detection have been developed during this research program. The most obvious approach is to test the collinearity of the measured color vector $\vec{c}$ with a reference vector $\vec{c}_0$ in the U, V system. However, using a conventional 8 MHz PC/AT system, even with an arithmetic coprocessor, the required cycle time turns out to be too slow for an adequate resolution in time, because of the great number of time-consuming computations that have to be performed for each pixel.

However, the processing speed could be significantly increased by partitioning the color circle into distinct sectors as shown in Fig. 4. Points of the same hue class must lie within the same sector. These sector conditions can be used for a quick pre-filtering of data, and further color comparisons do not have to be performed for all pixels, but only for a limited number of points. Using this algorithm, the sampling rate could be increased by a factor of 2 to 10 compared to the collinearity test described above, depending on how many pixels fullfil the sector condition at the same time.

3.4 Accuracy of measurement

Two groups of parameters do influence the accuracy of color detection: on one hand, the quality of the optical components and the analog signal processing elements, on the other hand, the specific quantification errors during digitalization and the inherent inaccuracies of the color detection algorithm.

Even in the camera a limitation with respect to the maximum color saturation arises. This effect is strongly dependent on the equipment and can only be controlled by calibration experiments. A conventional consumer video camera yields a multiplex signal, where brightness and color information is coded (FBAS signal). Due to compatibility requirements with monochrome receivers, the color difference signals must be restricted in band with, leading to reduced color contrast and limited quality of the color detection. Nevertheless, this FBAS approach had to be used because it was necessary not to manipulate the video camera.

Electric coupling and interference in the transmission line between camera and frame grabbers constitute further sources of errors. Furthermore, the adaption interface for offset correction may have some influence on the color difference signals.

Within the frame grabber interfaces, both an amplitude quantification and a discretisation of the component's surface into a limited number of pixel areas take place. Given the fixed resolution of the frame grabbers (8 bit), the color detection error is reduced with increasing color saturation, because the input voltage range of the A/D-converters is used more efficiently when the length of the color vector $\vec{c}$ is larger. The areal resolution error depends mainly on camera, scale and memory depth of the image-processing system.

3.5 Calibration

However, the errors discussed above may be quantified by calibration runs, leading to a somewhat limited range of colors that can be detected with adequate accuracy and reproducibility under the present conditions of the measuring system.

The color detection system has to be calibrated for a particular surface temperature using a thin aluminium bar that is electrically heated at one end. At the midpoint, the bar is coated with TLC and a thermocouple is embedded under its surface. This setup approximates one-dimensional heat conduction with an orthogonal line of constant temperature propagating along the length of the bar. The surface is monitored by the color recognition system in order to determine the time when the monitoring position displays a specific color. The amplified thermocouple signal is sampled periodically by an A/D converter so that the surface temperature can be correlated with color hue. The conditions of the actual test run are approximated by placing the calibration bar between rotor and stator and by using the same studio lighting.

4 Non-steady measurement technique

4.1 Heat transfer model

To determine the local heat transfer coefficients in rotor/stator configurations that are typical for turbine disc cavities (Fig. 5), the entire rotor and a section of the stator are coated with thermochromic liquid crystals.

The rotor/stator system is exposed to a sudden step change in convecting fluid temperature and the local surface temperature response of TLC coating is monitored (Metzger and Larson 1986; Clifford and Jones 1983). This information can be converted into heat transfer data for any surface point by solving the non-steady heat conduction equation:

$$\frac{dT}{dt} = \frac{\lambda}{\varrho\, c_p}\left(\frac{\partial^2 T}{\partial x^2} + \frac{\partial^2 T}{\partial y^2} + \frac{\partial^2 T}{\partial z^2}\right) \tag{2}$$

The disc can be considered to be a semi-infinite medium, because with the geometry and testing time presently in use the depth of heating is considerably less than the disc thickness. Lateral conduction in the wall has been shown to have only a negligible effect upon the local surface temperature response (Metzger and Larson 1986). Therefore, the surface points can be regarded to be independent of each other. Under these assumptions, the system's response to a true step in fluid temperature at $t=0$ is given by

$$\frac{T_s(t)-T_0}{T_{ref}-T_0} = 1-\exp(Bi^2)\, erfc(Bi) \tag{3}$$

with

$$Bi = \frac{\alpha\sqrt{at}}{\lambda}.$$

By solving Eq. (3), a corresponding local Biot Number can be found for each detected temperature-time pair.

However, in practice, the rotor and stator surfaces do not experience a true step in fluid temperature because of the transient heating of the upstream regions. Because the system is linear with respect to the charging reference value $(T_{ref}-T_0)$, it is possible to superpose a set of elementary steps in T_{ref} to represent the actual temperature rise:

$$T_s(t)-T_0 = \sum_{i=1}^{N} U(t-t_i)\, \Delta T_{ref,i} \tag{4}$$

where

$$U(t-t_i) = 1-\exp(Bi^2)\, erfc(Bi)$$

$$\Delta T_{ref,i} = \begin{cases} T_{ref,i}-T_{ref,i-1} & i>1 \\ T_{ref,i}-T_0 & i=1 \end{cases}$$

and

$$Bi = \frac{\alpha\sqrt{\alpha(t-t_i)}}{\lambda}.$$

Assuming that the local heat transfer coefficients are temperature independent, Eq. (4) can be solved iteratively.

4.2 Selection of reference temperature

The reference temperature T_{ref} used in Eqs. (3) and (4) is the local fluid temperature at a specific point of the disc's surface. Only if the heat losses to the wall are small is it justified that a global value, for example the jet inlet temperature, be used as a reference. In this case, the local heat transfer data can be obtained by a steady energy balance (Metzger and

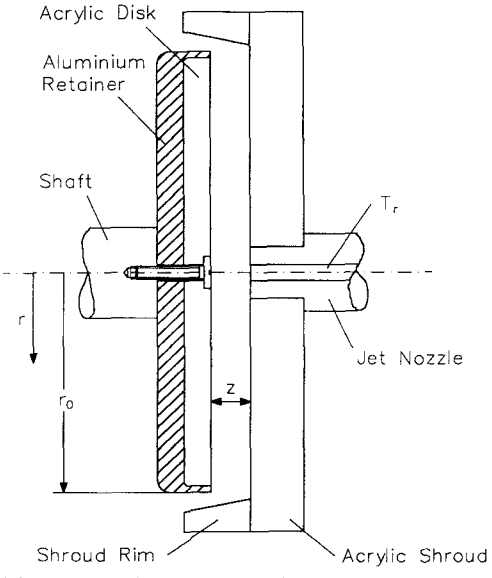

Fig. 5. Rotor/stator test-section

Larson 1986). With the present geometry, however, the variation of the wall temperature is significant and should not be neglected, leading to a more complex non-steady calculation scheme. Here the local reference temperatures are calculated by an explicit stepwise integration of the energy balance equation over the disc's radius (Hirsch 1987a). All these energy balance calculations do not take into account the ingress of ambient air into the rotor/stator cavity. This effect is most important in configurations without shroud rim and where the jet air supply is small compared to the disc pumping potential. In such cases, the gas temperatures in the cavity can be directly monitored by thermocouples and used as input for the heat transfer calculations (Schnetgoeke 1990).

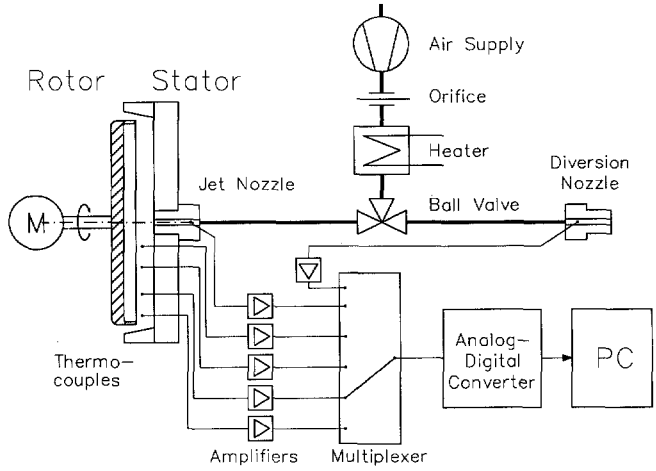

Fig. 6. Experimental setup

5 Results and discussion

5.1 Rotor/stator experimental setup

The rotor test surface is made of black acrylic plastic to improve the TLC color display. It is fitted into an aluminium retaining disc that is fastened to the rotating shaft. The stator disc, made of clear acrylic plastic, is mounted parallel to the rotor with a variable spacing. It can be equipped with a shroud rim to reduce ingress of ambient air into the cavity region (Fig. 5). The whole experimental apparatus is shown schematically in Fig. 6. The air supply is first metered using an orifice and then heated. Before the experiment starts, the air flow is guided through a ball diverter valve into a bypass with the test section remaining at ambient temperature. Only during the actual experiment is the test section exposed to the heated air stream.

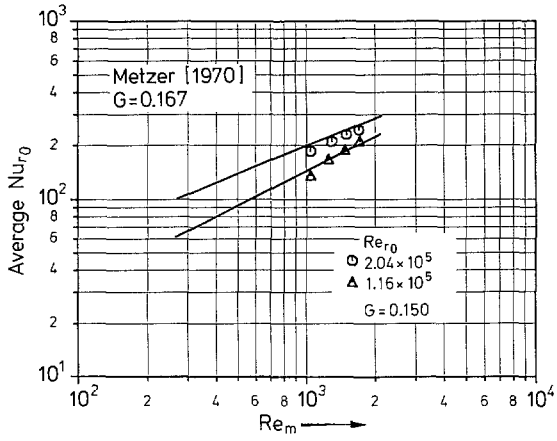

Fig. 7. Comparison with literature data

5.2 Comparison with literature data

The present parameter range are covered in a prior study by Metzger (1970). This study, however, only provides rotor averaged *Nu* data where the rotor was the only active heat transfer surface. In the present case, both rotor and stator are active surfaces and local heat transfer information is available. The TLC data had to be averaged an corrected to account for the heat transferred into the stator. Both methods are compared in Fig. 7. The agreement is good and verifies the current methodology and data acquisition.

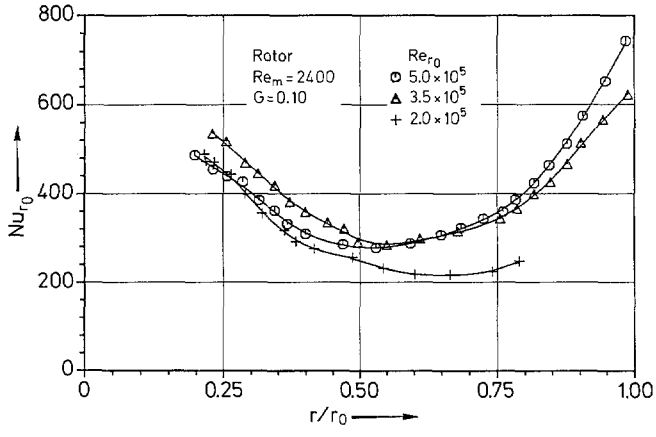

Fig. 8. Local rotor heat transfer data

5.3 Local heat transfer coefficients

In this paper, only some typical results are given to demonstrate the feasibility of the TLC technique. The rotor/stator heat transfer experiments preformed at the ITS have been reported elsewhere in detail (Bunker et al. 1990a; Bunker et al. 1990b). Figure 8 and 9 show the rotor and stator local heat transfer coefficients based on the local mean fluid temperature calculated by an energy balance. On the rotor two distinct regions exist: at small radii, jet impingement is dominant leading to high Nusselt numbers. As the flow propagates towards the outer regions of the rotor, the heat transfer intensity first levels off, but rises again when rotation be-

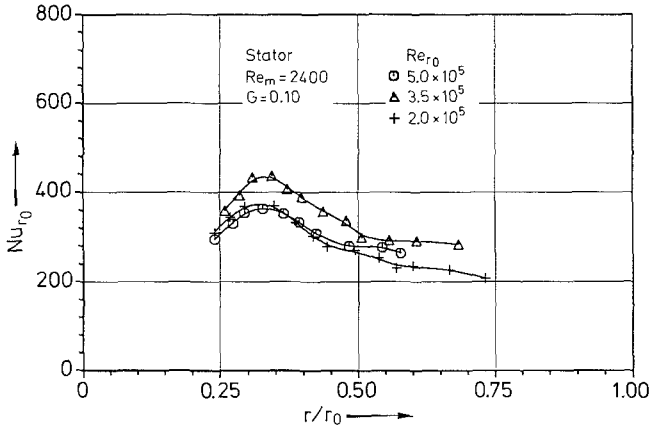

Fig. 9. Local stator heat transfer data

comes dominant. On the stator, the flow reattachment is of primary influence to the radial heat transfer variations. In this region, peak Nusselt numbers can be observed. Within this reattachment region, there is a monotonic decrease in Nu indicating a recirculation zone between jet injection and reattachment location on the stator.

6 Conclusions

The experimental technique using thin coatings of thermochromic liquid crystals as surface temperature indicators in a thermally transient experiment has proven its feasibility for detecting local heat transfer coefficients in rotor/stator systems for a broad range of parameters. Particularly, the computer-based color recognition system employed in the present study using color difference signals and the hue saturation coordinate system has been shown to be well-suited for a reliable on-line surface temperature detection.

Acknowledgements

This work was partially supported by the German National Science Foundation (Deutsche Forschungsgemeinschaft, DFG) within the larger context of the Sonderforschungsbereich 167 "High Intensity Combustors". Thanks are due to cand. mach. U. Schnetgoeke who was very helpful in performing the experiments.

References

Böttcher, B. 1972: Optische Eigenschaften cholesterinischer Flüssigkeiten – Hinweise für die Anwendungstechnik. CZ-Chemie-Technik, 1, 195–198

Bunker, R. S.; Metzger, D. E.; Wittig, S. 1990a: Local heat transfer in turbine disc-cavities. Part I: Rotor and stator cooling with hub injection of coolant. ASME Paper 90-GT-25

Bunker, R. S.; Metzger, D. E.; Wittig, S. 1990b: Local heat transfer in turbine disc-cavities. Part II: Rotor cooling with radial location injection of coolant. ASME Paper 90-GT-26

Clifford, R. J.; Jones, T. V. 1983: Techniques for obtaining detailed heat transfer coefficient measurements within gas turbine blade and vane cooling passages. ASME Paper 83-GT-58

Dibelius, G.; Radtke, F.; Ziemann, M. 1984: Experiments on friction, velocity and pressure distribution of rotating discs. In: Heat and Mass Transfer in Rotating Machinery (eds. Metzger, D. E.; Afgan, N. H.), pp. 117–130. New York: Hemisphere

Elser, W.; Ennulat, R. D. 1976: Selective reflection of cholesteric liquid crystals. In: Advances in Liquid Crystals (ed. Brown, G. H.), Vol. II, pp. 73–172. London: Academic Press

Hirsch, C. 1987a: Aufbau und Inbetriebnahme eines Versuchsstandes zur instationären Wärmeübergangsmessung an rotierenden Scheiben bei erzwungener Konvektion und Prallkühlung unter Nutzung thermochromer Flüssigkristalle als Temperaturindikatoren. Diplomarbeit ITS-Nr. 302, Institut für Thermische Strömungsmaschinen, Universität Karlsruhe

Hirsch, C. 1987b: Automated color recognition for liquid crystal heat transfer indication on complex surfaces using transient tests. M.S. thesis, Arizona State University

Metzger, D. E.; Larson, D. E. 1970: Heat transfer and pumping on a rotating disc with freely induced and forced cooling. J. Eng. Power 92, 342–348

Metzger, D. E.; Larson, D. E. 1986: Use of melting point surface coatings for local convective heat transfer measurements in rectangular channel flows with 90 deg Turns. J. Heat Transfer 108, 48–54

Oseen, C. W. 1933: The theory of liquid crystals. Transact. Faraday Soc. 29 219

Owen, J. M. 1984: Fluid flow and heat transfer in rotating disc systems. Heat and Mass Transfer in Rotating Machinery (eds. Metzger, D. E.; Afgan, N. H.), pp. 81–104. New York: Hemisphere

Schnetgoeke, U. 1990: Erweiterung eines Meßverfahrens zur Bestimmung der lokalen Wärmeübergangskoeffizienten in Rotor-Stator Systemen. Diplomarbeit ITS-Nr. 361, Institut für Thermische Strömungsmaschinen, Universität Karlsruhe

Seidel, R.; Burlisch, R. 1986: Vom Regenbogen zum Farbfernsehen. Berlin Heidelberg New York: Springer

De Vries, H. 1951: Rotatory power and other optical properties of certain liquid crystals. Acta Crystallographica 4, 219–226

Received July 1, 1991